Journal of Ethnopharmacology 148 (2013) 474–485

Contents lists available at SciVerse ScienceDirect

Journal of Ethnopharmacology

journal homepage: www.elsevier.com/locate/jep

Anti-oxidative stress effect of red ginseng in the brain is mediated by peptidyl arginine deiminase type IV (PADI4) repression via estrogen receptor (ER) β up-regulation

Eun-Hye Kim [a,1], In-Hye Kim [a,1], Mi-Jeong Lee [a], Cuong Thach Nguyen [a], Jung-Ah Ha [a], Soo-Cheol Lee [b], Sangdun Choi [b], Kwang-Tae Choi [c], Suhkneung Pyo [a], Dong-Kwon Rhee [a,*]

[a] School of Pharmacy, Sungkyunkwan University, Su-Won 440-746, South Korea
[b] Department of Molecular Science and Technology, Ajou University, Su-Won 443-749, South Korea
[c] HanbangBio Research Institute, Kyung Hee University, Su-Won 443-470, South Korea

ARTICLE INFO

Article history:
Received 4 February 2013
Received in revised form
5 April 2013
Accepted 18 April 2013
Available online 7 May 2013

Keywords:
Panax ginseng
Immobilization (IMO)
Oxidative stress
Peptidyl arginine deiminase type 4 (PADI4)
Estrogen receptor-β (ER-β)
Apoptosis

ABSTRACT

Aim of the study: Ginseng has been used as an anti-stress agent, and its active ingredient, ginsenoside, is similar in structure to estrogen. However, the effect of ginseng on the stressed brain is not completely understood. The aim of this study is to understand systematically how red ginseng (RG) affects gene expressions in the brain of immobilization (IMO) stressed mice to elucidate its underlying mechanism.
Materials and methods: For *in vivo* experiments, mice were stressed by immobilization for 30, 45, or 60 min, and gene expression in the mice brain was analyzed by microarray and system biology. Apoptosis was measured by terminal deoxynucleotidyl transferase-mediated digoxigenin-dUTP nick-end labeling (TUNEL) staining, and gene expression by Western blot or qPCR. For *in vitro* study, the SK-N-SH neuroblastoma cells were stressed by H_2O_2 exposure. The resultant cytotoxicity was measured by MTT assay, and gene expression by Western blot, ELISA, or qPCR.
Results: Microarray analysis of genes in IMO stressed mice brains showed that RG administration prior to IMO stress downregulated >40 genes including peptidyl arginine deiminase type 4 (PADI4). Interestingly, PADI4 was up-regulated by various stresses such as H_2O_2, acrylamide, and tunicamycin in neuroblastoma SK-N-SH cells but inhibited by RG. IMO stress and *in vitro* H_2O_2 stress depressed the estrogen receptor (ER)-β expression but not ERα. However, RG treatment increased ERβ expression both *in vivo* and *in vitro*. Comparative analysis regarding the networks by systems biology revealed that TNF-α plays a critical role in IMO stress, and the cell death associated network was much higher than other categories. Consistently, the IMO stress induced TNF-α and Cox-2 expressions, malondialdehyde (MDA), and cell death in the brain, whereas RG administration inhibited these inductions *in vivo*. siRNA and transient expression studies revealed that ERβ inhibited the PADI4 expression.
Conclusion: PADI4 could be used as an oxidative stress marker. RG seems to inhibit oxidative stress-inducible PADI4 by up-regulating ERβ expression in the brain thus protecting brain cells from apoptosis.

1. Introduction

Ginseng has been used and proven *in vivo* and clinically for anti-stress agents. Ginseng was shown to have anti-stress adaptogenic activity in foot electric shock stress test. Moreover, clinical trial also demonstrated that red ginseng (RG), steamed and dried, could help to maintain homeostasis in cold stress and work stress. Moreover, ginsenoside was identified as an active ingredient (Leung and Wong, 2010). Ginseng total saponin, ginsenosides Rg3 and Rb1 reduced polyamine levels, which were induced by immobilization-(IMO) stress in the brains of mice (Lee et al., 2006). The main ingredient of ginseng, Rb1, has a neuroprotective effect against ischemia (Lim et al., 1997), glutamate-induced neurotoxicity (Kim et al., 1998), seizures (Lian et al., 2005a), and neurodegeneration (Lian et al., 2005b). Growing evidence supports importance of estrogen in neuroprotective effect against acute injury and oxidative damages in brain by both estrogen receptor (ER)-dependent and ER-independent mechanisms (Simpkins et al., 2012). Rg3 in fermented red-ginseng has a neuroprotective effect and an anti-stress effect (Kim et al., 1998). Ginsenoside is structurally similar to glucocorticoid or estrogen since ginsenosides Re and Rg1 are functional ligands of the glucocorticoid receptor

Abbreviations: RG, Red Ginseng; IMO, Immobilization; MDA, Malondialdehyde; PADI4, peptidyl arginine deiminase type 4; TLR4, Toll Like Receptor 4..

* Corresponding author. Tel.: +82 31 2907707; fax: +82 31 2907727.
E-mail addresses: dkrhee@skku.edu, dkrhee4818@hanmail.net (D.-K. Rhee).

[1] Eun-Hye Kim and In-Hye Kim contributed equally.

0378-8741/$ - see front matter © 2013 Elsevier Ireland Ltd. All rights reserved.
http://dx.doi.org/10.1016/j.jep.2013.04.041

whereas ginsenosides Rb1 and Rh1 are functional ligands of the ER. Most ginsenosides share a dammarane triterpenoid structure with a four trans-ring rigid steroid skeleton (Leung and Wong, 2010). Ginseng was also shown to activate ER in breast cancer cells *in vitro* but not *in vivo* (Shim and Lee, 2012).

Physical stressors such as IMO, cold swim, and electric foot shock produce oxidative damage to membrane lipids in the brain (Liu et al., 1996). However, most of the ginseng and ginsenosides studies focused on biochemical parameters such as plasma glucose, cholesterol, serum corticosterone (Rai et al., 2003), plasma interleukin-6 (Kim et al., 2003), proinflammatory cytokines (IL-1β, IL-6, and TNF-α) (Joo et al., 2005), malondialdehyde levels (Voces et al., 2004), free radical scavenging activity *in vitro* (Kang et al., 2006), and the anti-inflammatory and anti-apoptotic effect of RG (Pannacci et al., 2006). Also, the glutathione level and superoxide dismutase activity in substantia nigra were determined in the brains of mice (Chen XC et al., 2005). Moreover, ginseng was found to increase the expression of toll like receptor 4 (TLR4) and the release of cytokines (Pannacci et al., 2006). However, the effect of ginseng on gene expression levels in the stressed brain remains unknown. Therefore, the aim of this study was to analyze how RG affected gene expressions in the brains of immobilized mice by systems biology. Furthermore, we investigated the role of RG as an anti-stress agent, which have neuroprotective activity during IMO stress.

2. Material and methods

2.1. Cells, animals, immobilization stress, RG, and treatment

Human neuroblastoma SK-N-SH cells (ATCC HTB-11) were cultured in RPMI 1640 (Lonza, USA) media containing 10% FBS, 1% penicillin–streptomycin (10000 U penicillin/ml, 10000 μg streptomycin/ml), 1 mM HEPES, 1 mM sodium pyruvate, 4.5 g/L glucose, 1.5 g/L bicarbonate, 2 mM L-glutamine at 37 °C, 5% CO_2. RG extract (Korean Ginseng Corporation, Korea) was manufactured by Korea Ginseng Corporation (Seoul, Korea) from roots of 6-year-old red ginseng, *Panax ginseng* Meyer, harvested in Republic of Korea. RG was made by steaming fresh ginseng at 90–100 °C for 3 h and then drying at 50–80 °C. To prepare RG water extract, RG was extracted at 85–90 °C for 8 h of circulating hot water three times. Yield of RG extract from RG was 75%. The water content of the pooled extract was 36% of total weight.

RG extract contains major ginsenoside—Rb1 4.62 mg/g, Rg2: 3.21 mg/g, Rg3: 3.05 mg/g, Rc: 2.41 mg/g, Rb2: 1.83 mg/g, Rf: 1.21 mg/g, Re: 0.93 mg/g, Rd: 0.89 mg/g, Rg1: 0.71 mg/g, and other minor ginsenosides (Supplementary Table S1). RG stock was prepared at 10 mg/ml in phosphate buffer saline (PBS, pH 7.4) and diluted with RPMI 1640 media containing 10% FBS and 2% penicillin–streptomycin to 1 mg/ml just prior to use and sterilized by filtration with a 0.22 μm bottle top filter (Nalgene, USA).

Male ICR mice (20–25 g) were housed in a temperature-controlled environment (temperature 21 ± 2 °C, humidity 60 ± 10%) under 12-h dark:12-h light cycle under the condition where food and water were freely available. All experiments conformed to the animal care guidelines of the Korean Academy of Medical Sciences, and all efforts were made in order to minimize their suffering. Stress procedures were approved and monitored by the ethical committee of SungKyunKwan University.

For stress experiments, mice were immobilized for 30, 45, or 60 min in a tightly fitted, 50 ml conical tube. At the end of the stress period, the mice were sacrificed by cervical dislocation, and the brain was rapidly removed and frozen. Animals that were set free in their home cage in the absence of any stressors served as controls (the normal control group). Mice were divided into three groups: non-treated (no stress), no treat+stress, RG+stress. The non-treated group was used as a control. The stress+no treat group was administrated only PBS. Lastly, the RG+stress group was administered 50 or 100 mg/kg of RG (red ginseng extract, Korean Ginseng Corporation, Korea) orally twice a day for 1 week. The mice began fasting on the evening of the 7^{th} day and were sacrificed 3 h after the last administration of RG on the morning of the 8th day.

For *in vitro* work, a filtered RG solution was further diluted with RPMI 1640 media to make 1 mg/ml prior to RG treatment. In addition, cells were treated with RG for 48 h.

2.2. Determination of lipid peroxidation

The lipid peroxidation was determined by measuring malondialdehyde (MDA) as previously described (Buege and Aust, 1978). Mice brains were homogenized in PBS, and 0.2 ml of brain homogenate was mixed with 0.2 ml of 8.1% (w/v) sodium dodecyl sulfate (SDS), 1.5 ml of 20% acetic acid (pH 3.5), 0.5 ml of 0.5% 2,6-di-tert-butyl-4-methylphenol (Sigma), and 1.5 ml of 0.8% 2-thiobarbituric acid. The mixture was incubated at 100 °C in a water bath for 30 min and cooled to room temperature for 30 min, centrifuged at 3600 *g* for 10 min. Subsequently, supernatant was used in order to determine MDA concentration at 535 nm by a spectrophotometer. The results are expressed as nmol MDA/mg protein.

2.3. MTT assay

Cell viability was determined by the MTT assay, which assesses mitochondrial function and correlates with cell viability (Musser and Oseroff, 1994). SK-N-SH cells were seeded in a 12 well plate with 4×10^4 cells per well in 1 ml of RPMI 1640 media. After overnight culture, cells were treated with RG for 2 h. The control was treated with RPMI 1640 media only. After 48 h incubation, cells were treated with H_2O_2 (0.5 mM for 2 h), supernatant was washed off, and the cells were further washed with PBS. Then, 1 ml of RPMI 1640 and 250 μl of MTT (2 mg/ml) were added into the culture, and the plate was incubated for 3 h at 37 °C with 5% CO_2. After removing supernatant, 3 ml of DMSO was added and purple formazan was dissolved completely with DMSO for 15 min followed by reading absorbance at 540 nm with an ELISA Reader. Each experiment was done in triplicate.

2.4. Purification of total RNA

Total RNA of the mouse brain or tissue cultured cells was isolated by using a TRIzol reagent (Invitrogen, USA) and purified using the RNeasy mini kit (Qiagen, USA) according to the manufacturer's instructions. RNA quality was measured by a spectrophotometer.

2.5. Microarray

Microarray hybridization, washing, and scanning were performed according to the manufacturer's protocol (Mouse Ref-8 Expression BeadChip Kit, Illumina). The list of genes is available through the Gene Expression Omnibus (http://www.ncbi.nml.nih.gov/geo) under the accession number GPL7245. All microarray data are deposited in ArrayExpress under accession number E-MTAB-856. The hierarchical clustering program used is implemented in the Multiple Experiment Viewer (http://www.jcvi.org/cms/research/software/).

2.6. Pathway analysis

The functional analysis algorithm from Ingenuity Pathway Analysis (IPA; Ingenuity Pathway Analysis Systems, www.ingenuity.com)

was used to identify the biological functions and/or diseases that were most significant to the data set. Each gene symbol was mapped to its corresponding gene object in the Ingenuity Pathways Knowledge Base. The networks regarding these genes were algorithmically generated based on their connectivity and assigned a score. Fold change was analyzed by either the ratio between the RG-treated and RG-non-treated group normalized to the control group or the RG-treated group normalized to the RG-non-treated group.

2.7. Real-time PCR

Total RNA was reversely transcribed to complementary DNA by M-MLV RT (RexGene biotech, Korea). All PCR primer pairs were designed for mRNA sequencing within 200 bp; PADI4, 5'-GGG TGA GTT CTT GAG CTT TG-3' (forward) and 5'-TCT TGA GTC CTT CGA ACA GT-3' (reverse); COX-2, 5'-AGA AGG AAA TGC CTG CAG AA-3' (forward) and 5'-GCT CGG CTT CCA GTA TTG AG-3' (reverse); β-actin, 5'-TGG AAT CCT GTG GCA TCC ATG AAA-3' (forward) and 5'-TAA AAC GCA GCT CAG TAA CAG TCC G-3' (reverse). Relative quantification of select mRNA was performed on 20 μl of cDNA using the Applied Biosystems StepOne and StepOnePlus Real-Time PCR Systems and the TaqMan Gene Expression Master Mix (Applied Biosystems, USA) according to the manufacturer's instructions. GAPDH and PADI4 probes were purchased from Bosung science (Korea).

The real-time PCR conditions were optimized to comprise an initial denaturation step of 10 min at 95 °C, followed by 40 cycles of 95 °C for 10 s, 55 °C for 15 s and 72 °C for 20 s. All samples were analyzed in quadruplicate. Data were analyzed using the ΔΔCT method in reference to β-actin (housekeeping gene), which was used as a control. This experiment was performed 3 times and statistics were analyzed by ANOVA.

2.8. DNA nick-end labeling

To assess apoptotic cells in the brain, terminal dexynucleotidyl transferase-mediated digoxigenin-dUTP nick-end labeling (TUNEL) staining was performed. Mice were fed RG extract for 7 days followed by IMO for 45 min. The brain was extracted and immediately fixed with 10% formalin (Sigma) after washing with PBS. Sectioned slides were assessed by TUNEL staining according to the manufacturer's protocol (*In situ* cell death detection kit; Roche Diagnostics, Basel, Germany). Under microscopy, the number of TUNEL-positive cells was counted per brain section. Numbers are apoptotic cells in randomly chosen histological fields of high-magnification (× 40). At least 2 representative areas were analyzed per sample.

2.9. Western blot analysis

Cells were collected by centrifugation after washing with PBS, and resuspended in a RIPA buffer (50 mM Tris–HCl pH 7.4, 0.5% sodium deoxycholate, 0.1% SDS, 150 mM NaCl, 1 mM EDTA, 1 mM PMSF and 1 × protease cocktail inhibitor). Cells were lysed by sonication and cell lysates were harvested after centrifugation at 12000 rpm, 4 °C for 15 min. The amount of protein was determined by Bradford assay. 30–40 μg of protein was used for Western blot analysis. Proteins separated by 10% or 15% SDS-PAGE were electroblotted onto a polyvinylidene difluoride (PVDF) membrane (Millipore, USA). The protein transferred membrane was incubated in a blocking buffer (7% skimmed milk, in TPBS [PBS, 0.1% Tween 20]) at room temperature on a shaking incubator for more than 1 h. After 3 times washing with TPBS, the membrane was incubated in a primary antibody (1:1000) for 1 h at room temperature. Primary antibodies comprising PADI4 (Abcam, USA), p-p53, caspase3 (Santacruz, USA), β-actin (Sigma), JNK and p-JNK (Cell signaling, USA) were purchased. After extensive washing, a secondary antibody (HRP-conjugated anti-IgG antibody, 1:5000 or 1:10000 anti-rabbit, anti-mouse, Sigma) was treated for 1 h. After washing, a detection reagent (Power Optic-ECL Western blotting Detection reagent, Animal genetics Inc., Korea) was added to the membrane and the film was developed.

2.10. ELISA assay

After IMO stress, whole brains were collected and homogenized, and 0.5% hexadecyltrimethylammonium bromide was added to the homogenized brain samples. After 3 rounds of freeze–thawing cycles, samples were sonicated and centrifuged at 14000 rpm, 4 °C, for 20 min. The supernatant (100 μL) was used for TNF-α ELISA assay (BD, USA) as per the manufacturer's instruction. Absorbance was measured at 450 nm after incubation in a lightproof condition for 20 min.

2.11. Transfection

To knock down PADI4 or ERβ expression by siRNA, 100 nM of siRNA (Genolution Phamaceuticals Inc., Korea) was added to 250 μL of serum free RPMI 1640 media without antibiotics, to which 5 μL of transfection reagent (TransIT-TKO, Mirus, USA) had been added and incubated for 20 min at room temperature. SK-N-SH cells (3×10^5 cells/well) were cultured in 6 well plates overnight, washed once with serum free media without antibiotics, and replaced with 1 ml of serum free media containing antibiotics. Subsequently, the transfection reagent containing siPADI4 or siERβ was added to the cell culture and incubated for 24 h. As a control, cells were transfected with MOCK siRNA. After incubation for 24 h, siRNA was removed and replaced with a new complete media containing 1 mg/ml RG (cells in RPMI 1640 media alone were used as a control) for 48 h. Subsequently, cells were washed with PBS twice, and exposed to 0.5 mM H_2O_2 for 2 h followed by washing and lysis.

For transient transfection with the ERβ, SK-N-SH cells (3×10^5 cells) were transfected with either a full-length hERβ expression plasmid (gift from Dr. M. Muyan at University of Rochester (Li et al., 2004)) or mock (hERβ plasmid was digested with *Pst*I restriction enzyme to delete 402 bp) by using *Trans*TKO Tranfection Reagent (Mirus, USA) for 24 h. The cells were then treated with 1 mg/ml of RG for 48 h or RPMI 1640 alone as a control. Subsequently, the cells were exposed to 0.5 mM H_2O_2 for 2 h. Protein was isolated from whole-cell lysates with the previously described RIPA buffer and 30 μg of protein was subjected to Western blot on 10% SDS-PAGE gel using ERβ antibody.

2.12. Statistical analysis

Data was analyzed by analysis of variance (ANOVA) followed by Dunett's *t*-test for comparisons between groups. Significance was accepted when $P < 0.05$ ($^*P < 0.05$; $^{**}P < 0.01$; $^{***}P < 0.001$). Data is expressed as median ± standard deviation for three to five independent experiments.

3. Results

3.1. Effect of RG on gene expression in the IMO-stressed brains of mice

As a preliminary *in vivo* study, we determined the RG dose effective for anti-IMO stress using MPO activity as an indicator. When RG (5, 25, and 100 mg/kg) was orally administered for 1 week followed by IMO-stress, administration of RG inhibited

MPO activity dose-dependently (60%, 40% and 30% of the IMO stressed control, respectively). Thus 100 mg/kg of RG was the most effective dose for repression of MPO activity (data not shown). Moreover, oral administration of RG extract 2000 mg/kg/day (approximately 200 times clinical doses) to mice for 2 weeks before mating to gestational day 18 did not show any considerable developmental toxicities such as abnormal fetal body weights, dysfunctional embryonic implantation or increased mortality (Shin et al., 2010). Therefore the dose we used is considered safe in our experiments.

Since IMO stress induced oxidative stress and leads to oxidative injury (Oishi et al., 1999), the IMO stress condition was optimized by determination of MDA levels in the IMO stressed brain. The MDA level was increased to 9-fold as compared to the non-stressed control after exposure to IMO stress for 30 min and 1 (data not shown). To determine the effect of RG on gene expression in the IMO-stressed brains of mice, microarray analyses were performed. Changes in gene expression between the normal group and the IMO stressed group were compared using a statistical criteria of ≥2-fold. Microarray analysis results showed that 104 genes including Apg31 (Atg3 autophagy-related 3), Slc4a1 (solute carrier family 4 anion exchanger member), PADI4 (peptidyl arginine deiminase type IV), and Rapgef5 (Rap guanine nucleotide exchange factor 5) were up-regulated more than 2 fold by IMO stress compared to the normal group. Of those genes, PADI4 was induced significantly higher by IMO stress than the normal group. However, these gene expressions were decreased by the RG pre-treatment (Supplementary Fig. S1B, Supplementary Table S2).

3.2. Repression of PADI4 by RG

To confirm microarray data, real-time quantitative PCR was performed. IMO stress induced the PADI4 gene significantly (72.5-fold), but the RG pre-pretreatment repressed it to the normal level (Fig. 1A) demonstrating that PADI4 was induced by IMO stress but was reversed by the RG pretreatment.

To confirm the anti-stress effect of RG further *in vitro*, cells were pre-treated with RG dose-dependently for 2 h and then exposed to H_2O_2 followed by determination of cell viability with MTT assay. Previously, various concentrations of RG on SK-N-SH

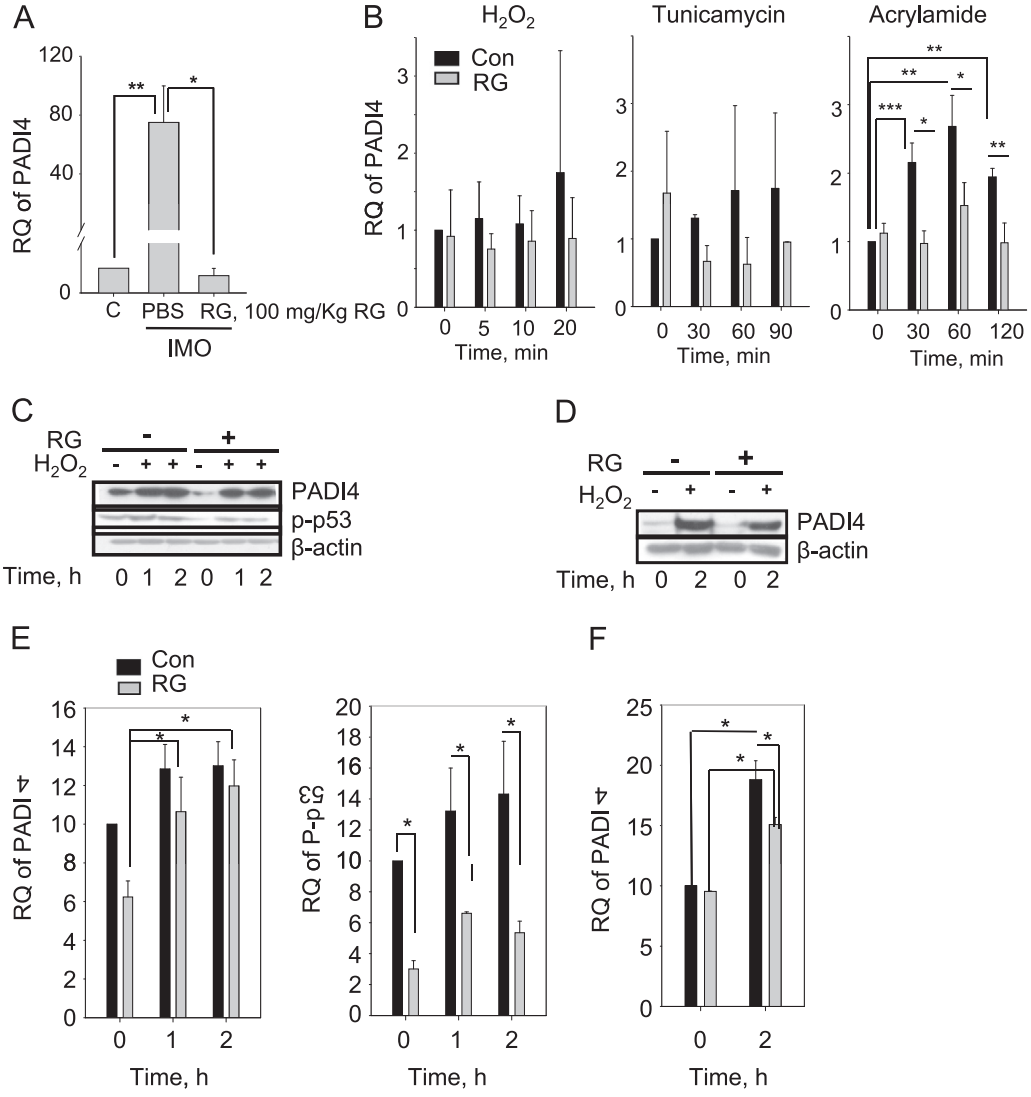

Fig. 1. Induction of PADI4 by stresses and reversion of the PADI4 induction by RG *in vivo* and *in vitro*. (A) Specified RG dose per mouse was administered orally for 7 days and then exposed to IMO stress for 45 min. (B) SK-N-SH cells were treated with various chemicals as described in the Methods. Gene expression levels of PADI4 were measured by real-time PCR (A, B). Data was normalized to β-actin. (C, D) 2×10^5 SK-N-SH (C) or 2×10^6 mouse peritoneal macrophage cells (D) were treated with 1 mg/mL of RG for 48 h (cells in RPMI 1640 media alone were used as a control). After treatment with 0.5 mM H_2O_2 for 1 or 2 h, cells were washed with PBS and lysed. Then cell lysates were analyzed by Western blot analysis. (E, F) Quantification of 2 independent experimental results from (C) and (D), respectively, was shown. Experiments were performed twice independently, and representative data from 2 experiments was shown. $^*P < 0.05$ *versus* RG-treated, by ANOVA.

neuronal cells were determined to test whether a certain concentration would affect cell viability (Kim et al., 2010). Incubation of various concentrations of RG with SK-N-SH cells for 24 h revealed that cell viability was not affected by <1 mg/mL of RG, but was decreased by >5 mg/mL of RG (Kim et al., 2010). The highest anti-stress effect of RG was shown at 1 mg/ml of RG compared to non RG-treated cells. Moreover, pre-treatment of cells with 1 mg/ml of RG for 48 h showed the highest repression of PADI4 expression as well as the highest viability of the cells (data not shown). Therefore, hereafter, cells were treated with RG for 48 h.

To further identify that PADI4 is induced by stresses in brain cells, the PADI4 gene expression was determined after several stresses. Human neuroblastoma SK-N-SH cells were treated with oxidative stressors H_2O_2 and acrylamide, or an endoplasmic reticulum stressor tunicamycin, and expression of PADI4 was determined by quantitative PCR. PADI4 expression was induced time-dependently by H_2O_2, acrylamide, and tunicamycin, whereas the induction of PADI4 was inhibited significantly by the RG pre-treatment compared to the non-RG pretreated control (Fig. 1B) demonstrating that PADI4 could serve as a stress marker and the RG pretreatment can repress stress-induced PADI4.

To corroborate PADI4 induction by oxidative stress at the protein level, cells were exposed to H_2O_2 for 1 or 2 h, and PADI4 level was determined by Western blot. After exposure to H_2O_2, PADI4 level was significantly induced in both SK-N-SH cancer cells and primary peritoneal macrophages (Fig. 1C–F). However, pre-treatment with RG, PADI4 level was significantly inhibited in both SK-N-SH and primary macrophage cells (Fig. 1C–F), demonstrating that PADI4 is induced by oxidative stress in both cancer and normal cells, but RG represses PADI4 induction after exposure to stresses.

3.3. Comparative analysis of networks

To further investigate which pathway was affected in the brain by either IMO stress or RG treatment, the expression levels of each gene were analyzed by Ingenuity Pathway Analysis. Interestingly, when genes were compared between (1) normal control *versus* IMO stress, (2) normal control *versus* RG+IMO stress, (3) IMO stress *versus* RG+IMO stress, the highest significance was found in the cell death category (score 45, $P<0.001$) within the group

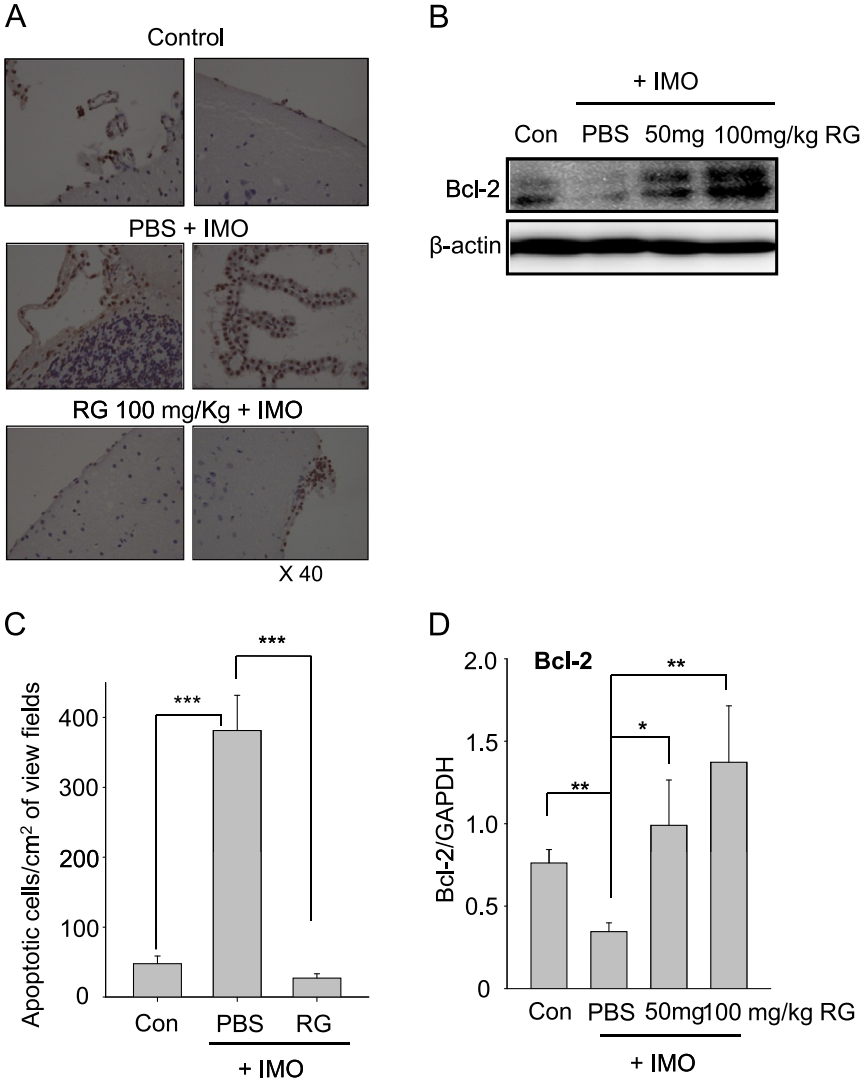

Fig. 2. Decrease of cell death by RG *in vivo*. (A) Mice were administered 100 mg/kg of RG for 1 week twice a day and the brains of mice were subject to TUNEL assay. Representative data from 3 mice samples are shown. Apoptotic cells were counted in randomly chosen x40 histological fields. (B) Mice were administered 50 and 100 mg/kg of RG for 1 week twice a day and then IMO stressed for 45 min. The protein was isolated from the brains of mice and then subjected to Western blot. Five mice per group were used for these experiments. Experiments were performed twice independently, and representative data from 2 experiments were shown. (C, D) Quantification of 2 independent experimental results from (A) and (B), respectively, was shown. Control, normal, and non-stressed control. $^{*}P<0.05$, $^{**}P<0.01$, $^{***}P<0.001$ *versus* control by two-way ANOVA.

comparing the normal control *versus* RG+IMO stress (data not shown).

Network 1. *Up-regulation of immune response-induced genes by IMO stress (Normal vs. IMO stress group)*—When pathway and network analysis was performed between the normal and the IMO stressed mice, it revealed a number of gene interactions in the brains of IMO stressed mice. Network analysis demonstrated that a red color depicts an increase of gene expression and a green color signifies a decrease of gene expression. Interestingly, TNF (tumor-necrosis factor), SMAD7, and HNF1A were found at the center of this network, and they comprised functional genes involved in immune and lymphatic system development and function, endocrine system disorders, and cell death (Supplementary Fig. S2A). Six genes including NFIX (Nuclear Factor I transcription factor), BST2 (interferon-induced cellular protein), TST (thiosulfate sulfurtransferase), HMGN3 (high mobility group nucleosomal binding domain 3), and RAPGEF5 (Rap guanine nucleotide exchange factor [GEF] 5) were up-regulated. NFIX genes were involved in cell growth and their activities were regulated by interleukin (IL).

Network 2. *Up-regulation of cell death associated genes in the IMO stressed mice (Normal vs. RG+IMO stress group)*—When the gene expressions of the RG pretreated group were compared with those of the normal group, the RG pre-administration up-regulated 14 genes (HOXA5, LGALS3BP, ITGB3BP, TGS1, DDB2, TFA2P2B, CITED2, CDKN1A, TP53INP1, CUGBP1, RAB7A, ZNF148, NCOA6, and SYT12) compared to those of the normal group, whereas it down-regulated 16 genes (RBM14, MEIS2, PBX1, SERPINH1, KLF6, BCCIP, NEUROD1, RSU1, RGM39, PCMT1, CREBBP, MED1, TCF7L2, FHIT, HNRNPA2B1, and SERCA). These results suggest that genes involved in cell death (HOXA5, LGALS3BP, ITGB3BP) were up-regulated by RG+IMO stress compared to the network 1 although it is not clear whether this change is due to RG pretreatment or IMO stress (Supplementary Fig. S2B). Therefore, network analysis was performed between IMO stress and RG+IMO stressed mice (network 3).

Network 3. *Upregulation of caspase-9 gene by RG pretreatment (IMO vs. RG+IMO stress group)*—When the gene expressions regarding the RG pretreated and IMO stressed group were compared with those of the IMO stressed group, Hsp90, Hsp70, HspA8, caspase, Casp9, JNK, and Akt were found at the center of the network (Supplementary Fig. S2C). The RG pretreatment up-regulated 5 genes including Caspase, CASP9, ITGB3BP, HBB, and DCX, which were involved in apoptosis, adhesion, hemoglobin β chain, as well as neuronal migration and differentiation. In

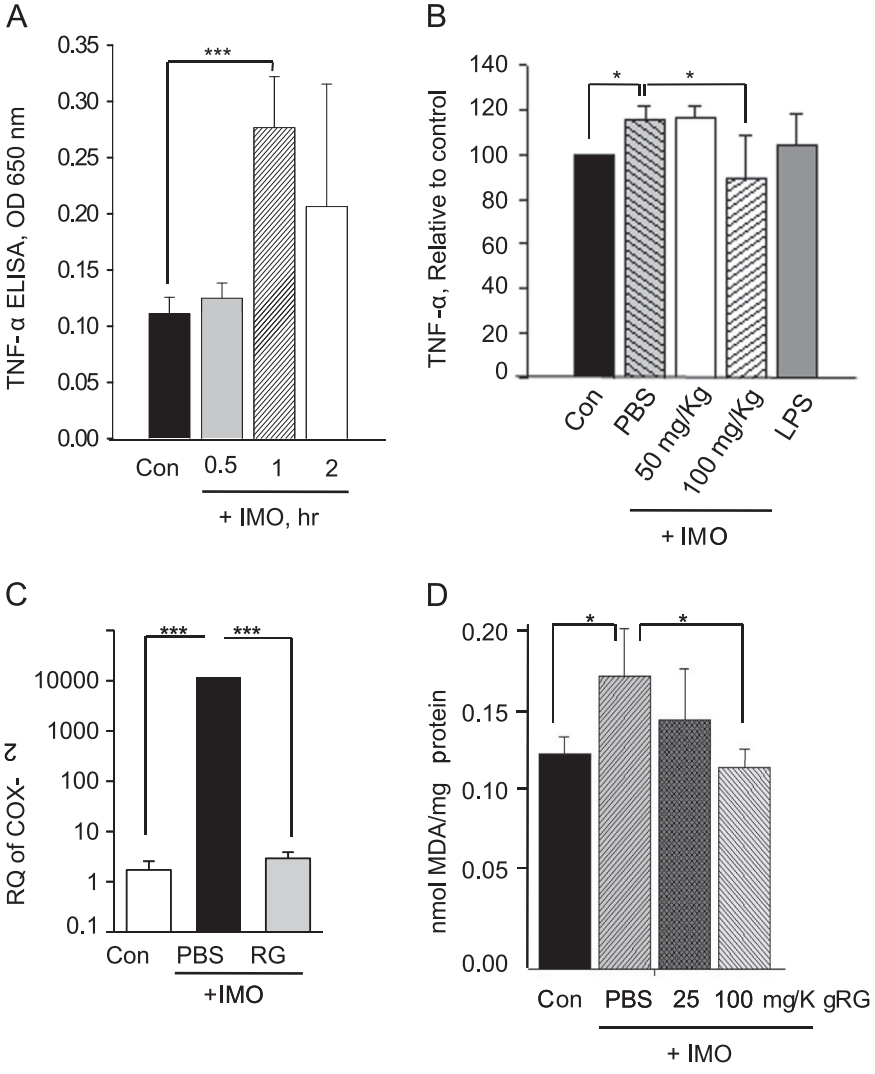

Fig. 3. Anti-inflammatory effect of RG in IMO stress. (A) After IMO, mice brain homogenates were used for TNF-α ELISA assay. (B) RG was administered for 1 week followed by IMO stress for 30 min. Mice brain homogenates were used for TNF-α ELISA assay. (C) RG 100 mg/Kg was administered for 1 week and followed by IMO stress for 45 min. The Cox-2 expression was determined by qPCR. (D) After administration of the specified RG dose per mouse for 1 week, mice were IMO stressed for 45 min, and the brain samples were homogenized and used for determination of malondialdehyde (MDA) concentration. Five mice per group were used for these experiments. These figures are representative of three independent experiments. Control, normal, and non-stressed control. $^{*}P < 0.05$, $^{**}P < 0.01$ *versus* control by two-way ANOVA.

contrast, RG pre-treatment down-regulated 23 genes including CD200, RETNLB, HspA5, HBD, Hsp70, and EIF4G2 (Supplementary Fig. S2C), which function in immune evasion, inflammatory response, and adhesion. Interestingly, caspase-9 induction by RG treatment did not increase caspase-3 expression, a downstream effector of caspase-9.

3.4. Inhibition of cell death by RG in vivo

Since IMO stress could induce cell death (Lee et al., 2006), nuclear changes in the brain after IMO stress was detected by TdT-mediated dUTP nick end labeling (TUNEL) assay. Positive staining of the TUNEL reaction was faintly detected in the nuclei of the control. After IMO stress, large numbers of positive staining in the neurons were localized in their cell bodies (Fig. 2A and C). However, the RG pre-treatment decreased the number of the staining to the non-stressed control (Fig. 2A and C) indicating that IMO stress produced a high level of cell death but the RG pre-treatment decreased the number of apoptotic bodies.

To corroborate that IMO stress could induce cell death in brain cells, expression of the pro-apoptosis gene, caspase-3, and the anti-apoptosis gene, bcl-2, was determined by Western blot analysis. Mice were divided into control, IMO stress, RG 50 mg +IMO, and RG 100 mg+IMO groups. Although caspase-3 expression was not changed significantly by IMO stress nor by RG pre-treatment (data not shown), bcl-2 expression in the IMO stressed group was decreased to 50% of the control group, whereas bcl-2 expression in RG 50 and 100 mg pre-administration was increased to 250% and 350%, respectively, for the IMO stress group (Fig. 2B and D). Consistently, in the oxidative-stressed condition *in vitro*, the active p-53 level was increased but pretreatment with RG suppresses p-53 induction (Fig. 1C and E). These results demonstrate that RG exhibits anti-apoptotic activity.

3.5. Anti-inflammatory effect of RG in IMO stress

Network analysis between the normal *versus* the IMO stress group showed up-regulation of immune response-induced genes by IMO stress, and TNF-α was found at the center of the network. Therefore, the TNF-α level was determined after IMO stress. IMO stress induced TNF-α significantly (Fig. 3**A**). In addition, RG pre-administration inhibited slightly the induction of TNF-α after IMO stress (Fig. 3B).

Since TNF-α induces ROS and other pro-inflammatory mediators, the anti-inflammatory effect of RG was determined by real time PCR using Cox-2 as an inflammatory marker (Clark et al., 2010). Results showed that IMO stress increased the Cox-2 expression significantly (152-fold higher) compared to that of the non-stressed control, whereas RG pre-administration depressed this induction near to the non-stressed control level (Fig. 3C) demonstrating that RG has significant anti-inflammatory activity *in vivo*.

To corroborate the anti-oxidative effect of RG, MDA levels were determined. Consistently, the MDA level was also significantly increased in IMO stressed mice whereas, it was decreased by the RG pretreatment dose-dependently, and administration of RG 100 mg/kg significantly inhibited the increase of MDA to the normal level (Fig. 3D).

3.6. Repression of ERβ by oxidative stress

To further elucidate the action mechanism of ginseng on the brain, mice were IMO stressed and the ER activation was determined by Western blot. IMO stress inhibited ERβ expression after IMO stress for 1 h but 100 mg/kg of the RG administration reversed the ERβ repression (Fig. 4A). However, IMO stress did not affect the ERα level, and the RG pre-treatment also did not

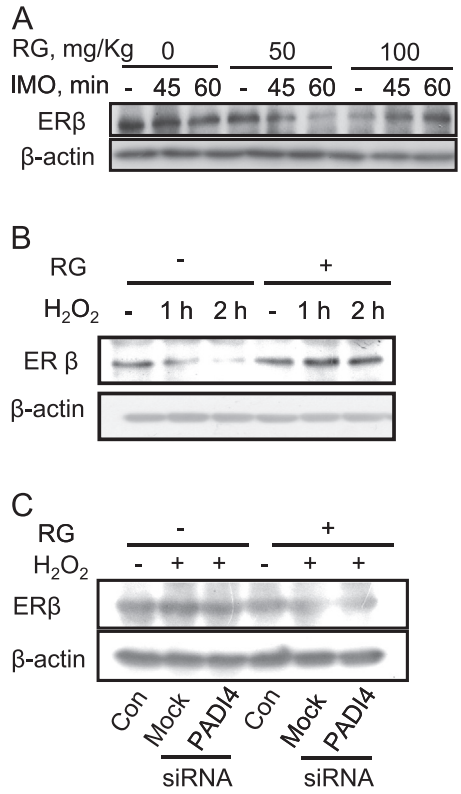

Fig. 4. Repression of ERβ by stress is reversed by RG. (A) Mice were administered 50 or 100 mg/kg of RG for 1 week, and IMO stressed for 45 min or 1 h. Subsequently, the ERβ level in the brain was determined by Western blot. (B, C) SK-N-SH cells were non-treated (B), or transfected with siPADI4 (C). Cells were further treated with 1 mg/ml of RG for 48 h or RPMI 1640 media alone. Subsequently, cells were exposed to 0.5 mM H_2O_2 for the time specified (B) or for 2 h (C), and lysed. Lysates were analyzed by Western blot analysis. This figure is representative of two independent experiments.

affect the ERα level (data not shown). Consistently, H_2O_2 stressed SK-N-SH cells showed a decrease of ERβ expression but the RG pre-treatment increased ERβ expression (Fig. 4B) demonstrating that ERβ is required for anti-stress activity in the brain and RG helps to induce ERβ expression.

To confirm the effect of RG on the ERβ expression of brain cells, siPADI4 RNA was used. In oxidative stress conditions, siPADI4 did not decrease ERβ levels significantly regardless of RG treatment compared to the mock experiment group (Fig. 4C) suggesting that PADI4 would not play a major role for regulation of the ERβ expression. These results demonstrate that oxidative stress suppressed the ERβ expression, and RG can reverse this repression.

3.7. ERβ prevents apoptosis in oxidative stress

To further investigate the regulation of ERβ and PADI4 expression in brain cells, cells were transfected with siERβ. Subsequently, cells were treated with RG, and exposed to H_2O_2 followed by determination of expressions regarding PADI4 and other apoptosis related genes by Western blot. In our previous experiments, we examined whether RG could protect the SK-N-SH cells from oxidative stress after treatment with H_2O_2. SK-N-SH cells were treated with 0.5 mM H_2O_2 for 0, 1, 2, and 4 h and viability of the cells was checked. The results (data not shown) indicated that RG protected the cells from oxidative stress after 2 and 4 h treatment with H_2O_2.

In general, p-JNK and p-P53 were detected within 30 min after 1 mM H_2O_2 treatment in human SH-SY5Y neuroblastoma cells (Ruffels et al., 2004), whereas p-JNK was induced by 0.4 mM H_2O_2

treatment for 1 h in the SH-SY5Y (Kwon et al., 2011) and PC12 neuronal cells (Li et al., 2011). Moreover, when p-JNK level was examined in SK-N-BE(2)-C cells after treatment with 0.25 mM H_2O_2, p-JNK level was induced at 15 min incubation but induced more significantly higher after 1 h. And p-JNK at 2 h incubation showed almost the same level as that of the 15 min incubation (Choi et al., 2009). These results demonstrate that induction of p-JNK depends on the H_2O_2 concentration and specific cell types. Therefore, in this study, the SK-N-SH cells were treated with 0.5 mM H_2O_2 for 2 h, which was the optimum for detection of apoptosis related proteins (such as Bcl-2, p-JNK, p-p53 etc.) expression. In the non-RG treated condition, siERβ increased the PADI4 level but decreased the pJNK level compared to the mock-transfected control indicating that ERβ depressed PADI4 expression but activates the JNK signaling pathway. However, RG treatment reversed PADI4 induction and pJNK repression by siERβ (Fig. 5A and B). Although, siERβ did not significantly affect the gene expressions in p53, p-p53, and JNK compared to the mock transfection regardless of RG treatment, siERβ increased the cleavage of caspase-3 to 185.7% and decreased Bcl-2 by 17.7% compared to the mock transfection in RG treated groups (Fig. 5A and B), suggesting that the ERβ expression could inhibit apoptosis, whereas PADI4 activates apoptosis. Consistently, RG treatment alone without oxidative stress showed higher PADI4 expression than the non-RG treated control (Fig. 5A and B).

To further corroborate the induction of PADI4 by ERβ siRNA and ERβ induction by RG, SK-N-SH cells were transiently transfected with ERβ expression plasmid and expressions of PADI4 and apoptosis genes were analyzed by Western blot. Consistently, PADI4 expression was inhibited by transfection with ERβ compared with the mutant ERβ-transfection in RG treated experiments (Fig. 5C) demonstrating that RG inhibits PADI4 expression via ERβ regulation. Although the tumor suppressor p53 level in the ERβ transfected RG-treated group was not significantly different from the mutant ERβ transfected RG-treated control, activated-p53, caspase-3, and pJNK were decreased by the ERβ transfected RG-treated group compared with the mutant ERβ transfected RG-treated control (Fig. 5C and D). Interestingly, Bcl-2, an anti-apoptotic factor, was not increased by ERβ-transfection compared to the mutant transfection (Fig. 5C). These results indicate that RG inhibits apoptosis through repression of p53, caspase-3, and JNK activation.

3.8. Repression of cell death via PADI4 by RG

Since the RG pretreatment suppressed PADI4 induction and reduced apoptosis upon exposure to IMO and other stresses, the repression of cell death could be due to the repression of PADI4 by RG. Moreover, PADI4 expression increased apoptosis in both rheumatoid arthritis (Hung et al., 2007) and cancer cells (Tanikawa et al., 2009), and p53 is a target of PADI4 (Tanikawa et al., 2009). Therefore, PADI4 induction could lead to p53 expression. To verify this possibility, the expression of active p53 (p-p53) was determined. Results showed that p-p53 was increased 30% and 50%, respectively, after exposure to H_2O_2 for 1 and 2 h compared to the non-stressed control (data not shown). In contrast, the RG pretreatment inhibited expression of p-p53 to less than 50% of the non-RG treated control (data not shown) indicating that oxidative stress induces p53 activation, but RG inhibited p53 activation after exposure to stresses.

TNF-α and ROS activate JNK (c-Jun N-terminal kinases), and JNK activates further p53 as well as other apoptotic factors (Circu and Aw, 2010). Therefore, to further investigate how RG affects cell death after PADI4 induction, SK-N-SH cells were transfected with siPADI4 prior to H_2O_2 stress, and expressions of apoptosis-associated genes and JNK activation were determined by Western blot. As a control, siPADI4 abrogated the PADI4 expression (Fig. 8A). Interestingly, in the non-stress condition, the RG pretreatment probably increased expressions of caspase-3, p53, and total JNK compared to the non-RG control (Fig. 6A) as a result of the overgrowth of the cells by the RG pretreatment and the subsequent overcrowding of stressful conditions. In the oxidative stress condition, siPADI4 inhibited expressions of p-JNK compared to the mock group, but increased Bcl-2 (Fig. 6A and B). These results indicate that oxidative stress induces PADI4, which subsequently activates p-JNK and down-regulates Bcl-2 leading to apoptosis. However, RG represses PADI4 induction and prevents apoptosis. Also, these results suggest that PADI4 might be an upstream regulator for caspase-3.

4. Discussion and conclusion

Clinically, stress is closely linked to various diseases via activation of the hypothalamus–pituitary–adrenal (HPA) axis (Reyes et al., 2003). Brain is the target of stress and stress hormones including glucocorticoids (Conrad and Bimonte-Nelson, 2010). Psycho-emotional stress induces the production of glucocorticoids, which subsequently promotes synthesis of adrenaline (Wong et al., 2008). Furthermore, excessive corticosterone release results in injury of several brain regions including the hippocampus (Patel et al., 2002).

In contrast, oxidative stress such as free radicals has been implicated as a major pathological mechanism of the brain disorders such as Alzheimer's disease, brain trauma, and Parkinson's disease (Basso et al., 2004). Since brain contains relatively large amount of iron and lipid content of myelin sheaths as well as high rate of oxidative metabolism and limited antioxidant capacity than the other organs, it is highly vulnerable to oxidative damage (Floyd, 1999; Herbert et al., 1994). In the brain, stress stimulates secretion of glucocorticoids, which augment the extracellular accumulation of glutamate in the hippocampus. Since glutamate can induce neuronal excitotoxicity and leads to TNFα release, this sequence results in translocation of NF-κB to neuronal nuclei and activation of the induction of iNOS and COX2, which are the two major enzymes responsible for the neurological damage. Subsequent generation of free radicals impairs DNA, oxidizes protein and lipid, and finally results in neural degeneration and cell death (Madrigal et al., 2006). Therefore, antioxidant agents comprising natural products have been developed as potential candidates for various degenerative disorders in the brain (Ghosh et al., 2011).

Estrogen including estradiol exerts a profound effect on brain function, and these effects are mainly mediated by ERα but not ERβ (Hewitt and Korach, 2003; Nogawa et al., 1998). However, most of the works on ERβ have been focused on brain function and behavior (Handa et al., 2012) except the ERβ expression is down-regulated by hypernatremia stress in the supraoptic nucleus within the brain (Jensen et al., 2010). Therefore, how ERβ is affected by stresses in the brain remains unknown. In this study, our results demonstrate that ERβ represses the PADI4 expression to antagonize stress in the brain.

Systems biology analyses demonstrated that IMO stress up-regulates the immune response associated genes in the brains of mice including TNF-α compared to the normal (network 1). Induction of immune-response associated genes could result in a disruption of homeostasis and eventually lead to a disease state. Indeed, IMO stress also induced cell death associated genes such as HOXA5 (apoptosis), LGALS3BP (cell death), and ITGB3BP (killing and adhesion), which demonstrated significantly higher induction than other genes. Therefore, it is highly likely that the induction of immune-response associated genes could lead to cell damage.

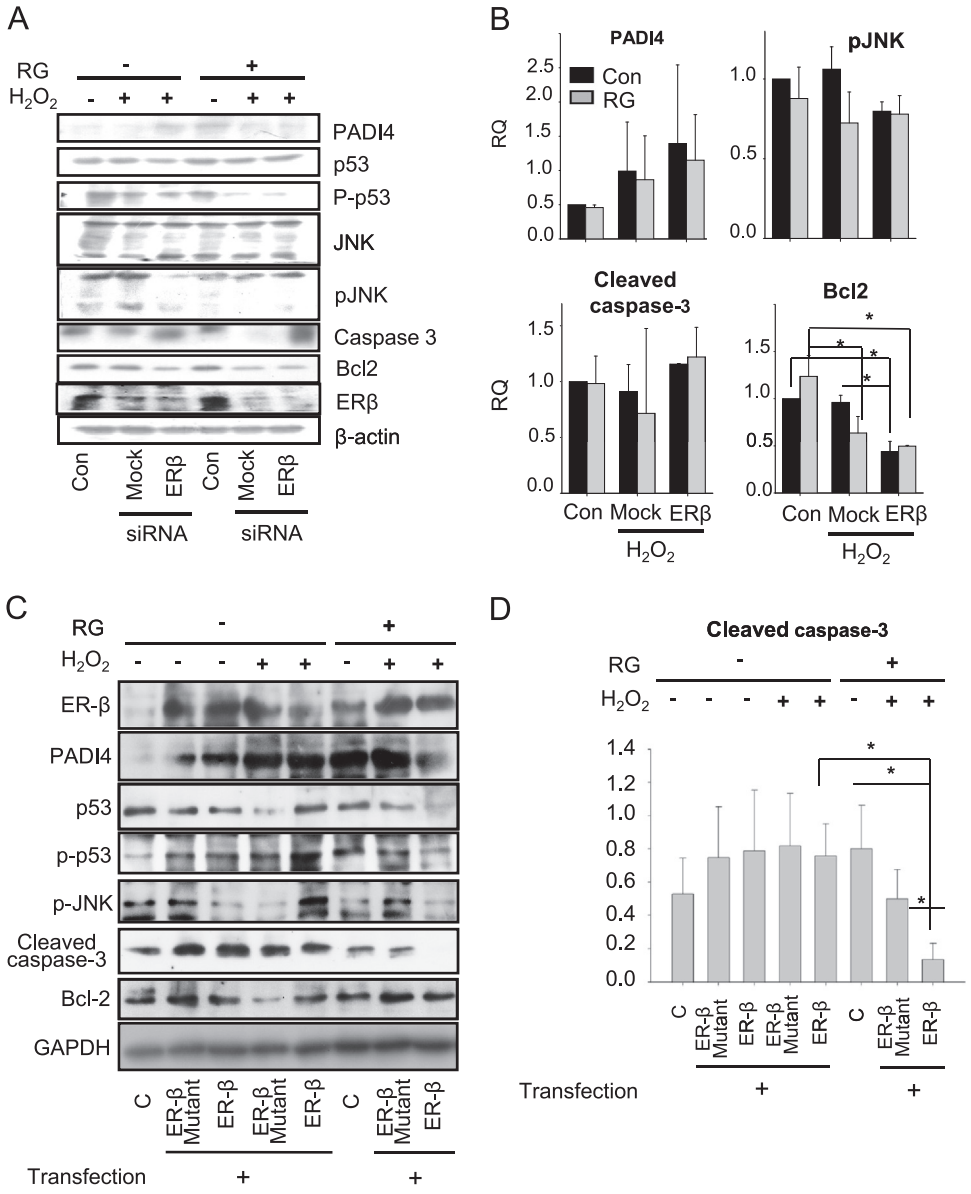

Fig. 5. Repression of apoptosis by ERβ. (A) SK-N-SH cells were transfected with siERβ, and subsequently further treated with 1 mg/ml of RG for 48 h or RPMI 1640 media alone. Then, cells were exposed to 0.5 mM H_2O_2 for 2 h, followed by lysis and Western blot analysis. Black bars were non-RG treated cells and gray bars were RG treated cells. Experiments were performed twice independently, and representative data from 2 experiments were shown. (B) Quantification of 2 independent experimental results from (A) was shown. (C) SK-N-SH cells were transiently transfected with ERβ expression plasmid. Subsequently, cells were treated with 1 mg/ml of RG for 48 h, and cell lysates were used for Western blot. The data are representative of at least 3 independent experiments. $^*P < 0.05$ *versus* RG-treated, by ANOVA.

Recently, increasing data suggest that there is an interaction between IMO stress and oxidative stress, and IMO stress was demonstrated to increase oxidative stress comprising MPO activity, lipid oxidation as well as other oxidative markers but not in a reverse way. In the chronic cold plus IMO stressed rat brain, oxidative stress parameters such as malondialdehyde (MDA), diene conjugate, and protein carbonyl levels were significantly increased compared with the non-stressed control (Kalaz et al., 2012). Also in the mice liver, long-term IMO resulted in significant increase of the oxidative stress markers such as a significant increase of MDA, an indicator of lipid peroxidation, as well as a significant reduction in catalase activity, which can indirectly indicate a high level of ROS, and subsequently cause substantial damage of intracellular macromolecules (Maksymchuk and Chashchyn, 2012). Consistently, the activities of glutathione peroxidase, superoxide dismutase, and the levels of lipid peroxidation were significantly increased with significant decrease of glutathione levels in the brain after IMO stressed groups (Ahmad et al., 2012).

Stress in the brain induces inflammatory responses and ends up with the release of inflammatory cytokines and the activation of neutrophils, and triggers oxidation of biomolecules and the severity of the disease. Thus, brain inflammation can contribute to cell damage (García-Bueno et al., 2008). Moreover, IMO stress increases the inducible isoform of NO synthase expression in rat brains, and its inhibition protects against stress-induced cell damage (Nogawa et al., 1998). Therefore, IMO stress could increase inflammatory responses through the induction of leukocytes in the brain, leading to tissue damages. In this study, RG treatment decreases MDA level compared to the IMO control group (Fig. 3D) suggesting that RG decreases damage to the brain by inhibiting lipid peroxidation, which is induced by IMO stress.

ERα and ERβ are usually tightly interrelated in the estradiol-dependent control for a particular brain function although

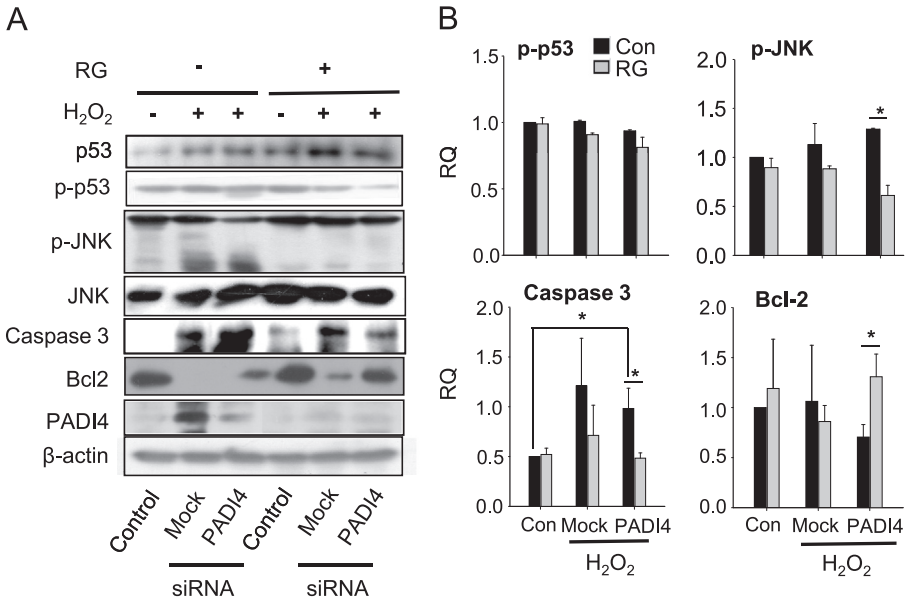

Fig. 6. Reversal of PADI4 induced gene expressions by RG. (A, B) Cells transfected with siPADI4 were treated with 1 mg/ml RG for 48 h, and exposed to 0.5 mM H_2O_2 for 2 h. Subsequently, cells were lysed, and then cell lysates were used for Western blot analysis (A). Quantification of 2 independent experimental results from (A) was shown (B). $^*P < 0.05$ *versus* RG-treated, by ANOVA.

reproduction is feedback principally controlled by estradiol through an ERα-dependent manner, and an important modulation by ERβ is also present (Handa et al., 2012). Moreover, ERα and ERβ could be synergistic or antagonistic within a particular neural network, *i.e.*, ERα enhances anxiety-like and aggressive behaviors, whereas ERβ suppresses them (Handa et al., 2012). Here, we found that the ERα expression *in vitro* was not affected by oxidative stress nor by RG treatment, thus ERα would not play a major role in oxidative stress in the brain. However, it does not rule out the interaction between ERα and ERβ. Further works on the interaction between ERα and ERβ in the brain warrant the underlying mechanism.

In eukaryotic cells, transcription is regulated by posttranslational histone modifications, such as acetylation, citrullination, methylation, phosphorylation, and ubiquitination. For example, histone Arg methylation is catalyzed by protein arginine methyltransferases (Bedford and Clarke, 2009), whereas PADI4 mediates histone Arg demethylation at a p21 promoter region (Li et al., 2008), which subsequently converts monomethyl-Arg to citrulline through demethylimination (Wang et al., 2004). Thus, PADI4 represses the expression of genes activated by estrogen and retinoic acid receptors (Wang et al., 2004), and serves as a p53 corepressor and represses the expression of p53 target genes p21/WAF1/CIP1 promoter (Li et al., 2008). Therefore, overexpression of PADI4 induces apoptosis mainly through cell cycle arrest in the G1 phase and a mitochondria-mediated pathway, suggesting an important role for PADI4 in immune cell differentiation and cell death. However, most of the PADI4 studies were concentrated on rheumatoid arthritis (RA), which is one of the most common chronic inflammatory syndromes [see review; (Anzilotti et al., 2010)]. Hence, PADI4 induction by a variety of oxidative stresses comprising IMO stress suggests that PADI4 could be a feasible marker for the oxidative stress response.

When gene expressions in a mouse's adrenal cortex were examined by microarray analysis after repeated IMO stress for 5 days, 168 genes were modulated by IMO stress (Kim and Lee, 2011). Although these 168 genes modulated by IMO were not the same as the genes we found in this experiment, the functions modulated by ginseng (apoptosis, cell cycle, immune response, inflammatory responses, and signal transduction) are similar to our results (nervous system development and function, cell death and immune response). These differences might be ascribed to IMO stress time (< 1 h *versus* consecutive 5 days) and/or different organs (adrenal cortex *versus* whole brain) used for microarray.

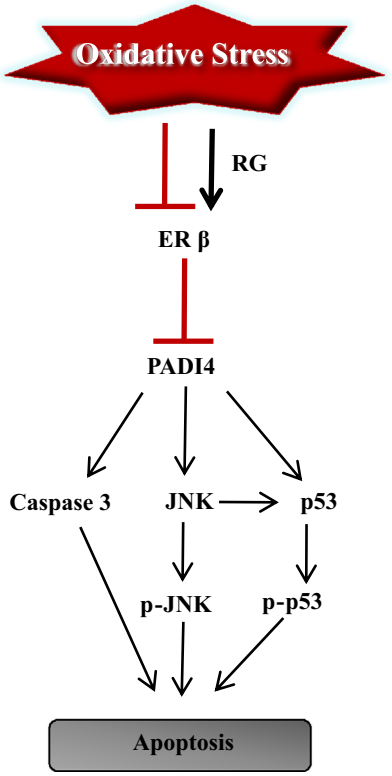

Fig. 7. Activation of ERβ by RG inhibits apoptosis in an oxidatively stressed brain. Oxidative stress inhibited ERβ, which is required for the activation of PADI4. PADI4 activation induces JNK phosphorylation and activates apoptosis related genes. RG induces ERβ but represses PADI4 thereby inhibiting apoptosis in the brain.

Collectively, oxidative stress inhibits ERβ and subsequently induces PADI4, which could result in the activation of downstream inflammation related genes and pro-apoptotic factors comprising

p53, caspase-3, and JNK. Since IMO and other stresses induce PADI4, PADI4 could be a stress marker. In contrast, RG suppressed the PADI4 expression via ERβ up-regulation, thus reversing the stress induced gene expression and subsequently inhibiting apoptosis by repressing p53, caspase-3 and JNK activation and by inducing Bcl-2 (Fig. 7).

Acknowledgments

This work was supported by the grant from the Korean Society of Ginseng funded by the Korea Ginseng Cooperation (2009-2011) and the Korea Science & Engineering Foundation (WCU R33-10045) to DKR, and also partly supported by the Basic Science Research Program through the National Research Foundation of Korea to SC (2010-0015356).

Appendix A. Supporting information

Supplementary data associated with this article can be found in the online version at http://dx.doi.org/10.1016/j.jep.2013.04.041.

References

Ahmad, A., Rasheed, N., Ashraf, G., Kumar, R., Banu, N., Khan, F., Al-Sheeha, M., Palit, G., 2012. Brain region specific monoamine and oxidative changes during restraint stress. Canadian Journal of Neurological Sciences 39, 311–318.

Anzilotti, C., Pratesi, F., Tommasi, C., Migliorini, P., 2010. Peptidylarginine deiminase 4 and citrullination in health and disease. Autoimmunity Reviews 9, 158–160.

Basso, M., Giraudo, S., Corpillo, D., Bergamasco, B., Lopiano, L., Fasano, M., 2004. Proteome analysis of human substantia nigra in Parkinson's disease. Proteomics 4, 3943–3952.

Bedford, M.T., Clarke, S.G., 2009. Protein arginine methylation in mammals: who, what, and why. Molecular Cell 33, 1–13.

Buege, J.A., Aust, S.D., 1978. Microsomal lipid peroxidation. Methods in Enzymology 52, 302–310.

Chen, X.C., Zhou, Y.C., Chen, Y., Zhu, Y.G., Fang, F., L.M., C., 2005. Ginsenoside Rg1 reduces MPTP-induced substantia nigra neuron loss by suppressing oxidative stress. Acta Pharmacologica Sinica 26, 56–62.

Choi, K., Kim, J., Kim, G., Choi, C., 2009. Oxidative stress-induced necrotic cell death via mitochondira-dependent burst of reactive oxygen species. Current Neurovascular Research 6, 213–222.

Circu, M.L., Aw, T.Y., 2010. Reactive oxygen species, cellular redox systems and apoptosis. Free Radical Biology & Medicine 48, 749–762.

Clark, I.A., Alleva, L.M., Vissel, B., 2010. The roles of TNF in brain dysfunction and disease. Pharmacology & Therapeutic 128, 519–548.

Conrad, C.D., Bimonte-Nelson, H.A., 2010. Impact of the hypothalamic-pituitary-adrenal/gonadal axes on trajectory of age-related cognitive decline. Progress in Brain Research 182, 31–76.

Floyd, R., 1999. Antioxidants, oxidative stress, and degenerative neurological disorders. Proceedings of the Society for Experimental Biology and Medicine 222, 236–245.

García-Bueno, B., Caso, J.R., Leza, J.C., 2008. Stress as a neuroinflammatory condition in brain: damaging and protective mechanisms. Neuroscience & Biobehavioral Reviews 32, 1136–1151.

Ghosh, N., Ghosh, R., Mandal, S.C., 2011. Antioxidant protection: a promising therapeutic intervention in neurodegenerative disease. Free Radical Research 45, 888–905.

Handa, R.J., Ogawa, S., Wang, J.M., Herbison, A.E., 2012. Roles for oestrogen receptor β in adult brain function. Journal of Neuroendocrinology 24, 160–173.

Herbert, V., Shaw, S., Jayatilleke, E., Stopler-Kasdan, T., 1994. Most free-radical injury is iron-related: it is promoted by iron, hemin, holoferritin and vitamin C, and inhibited by desferoxamine and apoferritin. Stem Cells 12, 289–303.

Hewitt, S., Korach, K., 2003. Oestrogen receptor knockout mice: roles for oestrogen receptors alpha and beta in reproductive tissues. Reproduction 125, 143–149.

Hung, H.-C., Lin, C.-Y., Liao, Y.-F., Hsu, P.-C., Tsay, G., Liu, G.-Y., 2007. The functional haplotype of peptidylarginine deiminase IV (S55G, A82V and A112G) associated with susceptibility to rheumatoid arthritis dominates apoptosis of acute *T* leukemia Jurkat cells. Apoptosis 12, 475–487.

Jensen, E.V., Jacobson, H.I., Walf, A.A., Frye, C.A., 2010. Estrogen action: a historic perspective on the implications of considering alternative approaches. Physiology & Behavior 99, 151–162.

Joo, S.S., Won, T.J., Lee, D.I., 2005. Reciprocal activity of ginsenosides in the production of proinflammatory repertoire, and their potential roles in neuroprotection *in vitro*. Planta Medica 71, 476–481.

Kalaz, E.B., Evran, B., Develi-Is, S., Vural, P., Dogru-Abbasoglu, S., Uysal, M., 2012. Effect of carnosine on prooxidant-antioxidant balance in several tissues of rats exposed to chronic cold plus immobilization stress. Journal of Pharmacological Sciences 120, 98–104.

Kang, K.S., Kim, H.Y., Pyo, J.S., Yokozawa, T., 2006. Increase in the free radical scavenging activity of ginseng by heat-processing. Biological & Pharmaceutical Bulletin 29, 750–754.

Kim, D.-H., Jung, J.-S., Moon, Y.-S., Sung, J.-H., Suh, H.-W., Kim, Y.-H., Song, D.-K., 2003. Inhibition of intracerebroventricular injection stress-induced plasma corticosterone levels by intracerebroventricularly administered compound K, a ginseng saponin metabolite, in mice. Biological & Pharmaceutical Bulletin 26, 1035–1038.

Kim, E.-H., Lee, M.-J., Kim, I.-H., Pyo, S., Choi, K.-T., Rhee, D.-K., 2010. Anti-apoptotic effects of red ginseng on oxidative stress induced by hydrogen peroxide in SK-N-SH cells. Journal of Ginseng Research 34, 138–144.

Kim, Y.C., Kim, S.R., Markelonis, G.J., Oh, T.H., 1998. Ginsenosides Rb1 and Rg3 protect cultured rat cortical cells from glutamate-induced neurodegeneration. Journal of Neuroscience Research 53, 426–432.

Kim, Y.O., Lee, S.W., 2011. Microarray analysis of gene expression by ginseng water extracts in a mouse adrenal cortex after immobilization stress. Journal of Ginseng Research 35, 111–123.

Kwon, S.-H., Kim, J.-A., Hong, S.-I., Jung, Y.-H., Kim, H.-C., Lee, S.-Y., Jang, C.-G., 2011. Loganin protects against hydrogen peroxide-induced apoptosis by inhibiting phosphorylation of JNK, p38, and ERK 1/2 MAPKs in SH-SY5Y cells. Neurochemistry International 58, 533–541.

Lee, S.H., Jung, B.H., Kim, S.Y., Lee, E.H., Chung, B.C., 2006. The antistress effect of ginseng total saponin and ginsenoside Rg3 and Rb1 evaluated by brain polyamine level under immobilization stress. Pharmacological Research 54, 46–49.

Leung, K., Wong, A., 2010. Pharmacology of ginsenosides: a literature review. Chinese Medicine 5, 20.

Li, W.-W., Gao, X.-M., Wang, X.-M., Guo, H., Zhang, B.-L., 2011. Icariin inhibits hydrogen peroxide-induced toxicity through inhibition of phosphorylation of JNK/p38 MAPK and p53 activity. Mutation Research 708, 1–10.

Li, P., Yao, H., Zhang, Z., Li, M., Luo, Y., Thompson, P.R., Gilmour, D.S., Wang, Y., 2008. Regulation of p53 target gene expression by peptidylarginine deiminase 4. Molecular and Cellular Biology 28, 4745–4758.

Li, X., Huang, J., Yi, P., Bambara, R.A., Hilf, R., Muyan, M., 2004. Single-chain estrogen receptors (ERs) reveal that the ERalpha/beta heterodimer emulates functions of the ERalpha dimer in genomic estrogen signaling pathways. Molecular and Cellular Biology 24, 7681–7694.

Lian, X.-Y., Zhang, Z.-Z., Stringer, J.L., 2005a. Anticonvulsant activity of ginseng on seizures induced by chemical convulsants. Epilepsia 46, 15–22.

Lian, X.-Y., Zhang, Z., Stringer, J.L., 2005b. Protective effects of ginseng components in a rodent model of neurodegeneration. Annals of Neurology 57, 642–648.

Lim, J.H., Wen, T.C., Matsuda, S., Tanaka, J., Maeda, N., Peng, H., Aburaya, J., Ishihara, K., Sakanaka, M., 1997. Protection of ischemic hippocampal neurons by ginsenoside Rb1, a main ingredient of ginseng root. Neuroscience Research 28, 191–200.

Liu, J., Wang, X., Shigenaga, M.K., Yeo, H.C., Mori, A., Ames, B.N., 1996. Immobilization stress causes oxidative damage to lipid, protein, and DNA in the brain of rats. The Federation of American Societies for Experimental Biology 10, 1532–1538.

Madrigal, J., García-Bueno, B., Caso, J., Pérez-Nievas, B., Leza, J., 2006. Stress-induced oxidative changes in brain. CNS & Neurological Disorders—Drug Targets 5, 561–568.

Maksymchuk, O., Chashchyn, M., 2012. The impact of psychogenic stressors on oxidative stress markers and patterns of CYP2E1 expression in mice liver. Pathophysiology 19, 215–219.

Musser, D.A., Oseroff, A.R., 1994. The use of tetrazolium salts to determine sites of damage to the mitochondrial electron transport chain in intact cells following *in vitro* photodynamic therapy with photofrin ii. Photochemistry and Photobiology 59, 621–626.

Nogawa, S., Forster, C., Zhang, F., Nagayama, M., Ross, M.E., Iadecola, C., 1998. Interaction between inducible nitric oxide synthase and cyclooxygenase-2 after cerebral ischemia. Proceedings of the National Academy of Sciences of the United States of America 95, 10966–10971.

Oishi, K., Yokoi, M., Maekawa, S., Sodeyama, C., Shiraishi, T., Kondo, R., Kuriyama, T., Machida, K., 1999. Oxidative stress and haematological changes in immobilized rats. Acta Physiologica Scandinavica 165, 65–69.

Pannacci, M., Lucini, V., Colleoni, F., Martucci, C., Grosso, S., Sacerdote, P., Scaglione, F., 2006. Panax ginseng C.A. Mayer G115 modulates pro-inflammatory cytokine production in mice throughout the increase of macrophage toll-like receptor 4 expression during physical stress. Brain, Behavior, and Immunity 20, 546–551.

Patel, R., McIntosh, L., McLaughlin, J., Brooke, S., Nimon, V., Sapolsky, R., 2002. Disruptive effects of glucocorticoids on glutathione peroxidase biochemistry in hippocampal cultures. Journal of Neurochemistry 82, 118–125.

Rai, D., Bhatia, G., Sen, T., Palit, G., 2003. Anti-stress effects of Ginkgo biloba and Panax ginseng: a comparative study. Journal of Pharmacological Sciences 93, 458–464.

Reyes, T.M., Walker, J.R., DeCino, C., Hogenesch, J.B., Sawchenko, P.E., 2003. Categorically distinct acute stressors elicit dissimilar transcriptional profiles in the paraventricular nucleus of the hypothalamus. Journal of Neuroscience 23, 5607–5616.

Ruffels, J., Griffin, M., Dickenson, J.M., 2004. Activation of ERK1/2, JNK and PKB by hydrogen peroxide in human SH-SY5Y neuroblastoma cells: role of ERK1/2 in H2O2-induced cell death. European Journal of Pharmacology 483, 163–173.

Shim, M.K., Lee, Y.J., 2012. Estrogen receptor is activated by Korean red ginseng *in vitro* but not *in vivo*. Journal of Ginseng Research 36, 69–175.
Shin, S., Jang, J.Y., Park, D., Yon, J.-M., Baek, I.-J., Hwang, B.Y., Nam, S.-Y., Yun, Y.W., Kim, K.-Y., Joo, S.S., Kim, Y.-B., 2010. Korean red ginseng extract does not cause embryo-fetal death or abnormalities in mice. Birth Defects Research: Part B, Developmental and Reproductive Toxicology 89, 78–85.
Simpkins, J.W., Singh, M., Brock, C., Etgen, A.M., 2012. Neuroprotection and estrogen receptors. Neuroendocrinology 96, 119–130.
Tanikawa, C., Ueda, K., Nakagawa, H., Yoshida, N., Nakamura, Y., Matsuda, K., 2009. Regulation of protein Citrullination through p53/PADI4 network in DNA damage response. Cancer Research 69, 8761–8769.
Voces, J., Cabral de Oliveira, A.C., Prieto, J.G., Vila, L., Perez, A.C., Duarte, I.D.G., Alvarez, A.I., 2004. Ginseng administration protects skeletal muscle from oxidative stress induced by acute exercise in rats. Brazilian Journal of Medical and Biological Research 37, 1863–1871.
Wang, Y., Wysocka, J., Sayegh, J., Lee, Y.-H., Perlin, J.R., Leonelli, L., Sonbuchner, L.S., McDonald, C.H., Cook, R.G., Dou, Y., Roeder, R.G., Clarke, S., Stallcup, M.R., Allis, C.D., Coonrod, S.A., 2004. Human PAD4 regulates histone arginine methylation levels via demethylimination. Science 306, 279–283.
Wong, D.L., Tai, T.C., Wong-Faull, D.C., Claycomb, R., Kvetňanský, R., 2008. Adrenergic responses to stress. Annals of the New York Academy of Sciences 1148, 249–256.